Malaysian Journal of Civil Engineering 30(2):296-312 (2018)

MODELING SINGLE BARRETTES AS ELASTIC SUPPORT BY CCT

Mahmoud El Gendy *, Hassan Ibrahim & Ibrahim El Arabi

Department of Civil Engineering, Faculty of Engineering, Port Said University, Egypt, 42526 Port Said, Egypt

*Corresponding Author: *mahmoud_gendy1@hotmail.com*

Abstract: Classical analyses of barrette foundation taking into account full interactions between barrette and the surrounding soil leads to a huge barrette stiffness matrix. Consequently, a large system of linear equations must be solved, especially for analyzing barrette group and barrette raft. To overcome this problem, a Composed Coefficient Technique (CCT) is developed for analyzing barrette. In the analysis, the elasticity of the barrette body is considered using the finite element method, while that of the soil elements is considered using flexibility coefficients. The compatibility between the vertical displacements of the barrette and the soil settlements at the soil-barrette interface is taken in the vertical direction only. This assumption is that the external load on the barrette head, which is expected to be heavy load, is applied in the vertical direction. For comparative examinations, the barrette elasticity is determined using either 1D or 3D finite elements. A series of examinations is carried out to verify the application for analyzing barrette by CCT. It was found that, treating the barrette as an elastic body and representing the barrette by either 1D or 3D finite elements, gives nearly the same results.

Keywords: *Soil structure interaction, deep foundation, barrette, settlement.*

Article history:
Received 28 July 2017
Received in revised form 20 Dec 2017
Accepted 1 May 2018
Published online 30 June 2018

1.0 Introduction

Heavy loaded structures such as bridges and high raise buildings generate huge axial loads and need to be rested on large-section supports of deep foundations such as barrette foundations. Classical analyses of large-section support as barrette foundation taking into account full interactions between barrette and the surrounding soil leads to a huge barrette stiffness matrix. Consequently, a large system of linear equations must be solved, and thus these analyses are time consuming even for the fast computers of today, especially for analyzing barrette group and barrette raft.

El Gendy, (2007), first proposed composed Coefficient Technique (CCT). He applied the technique on single pile, pile group and piled raft to reduce the size of the entire soil stiffness matrix. In this technique, the pile is treated as a rigid member having a uniform settlement for all nodes along its shaft and base. CCT enables to assemble pile coefficients in composed coefficients. This technique was examined and applied efficiently for many studies, some of them are those of Hattab, (2007); Reda, (2009); Rabiei, (2009, 2010, 2016); Kamash, (2009, 2012); Kamash *et al*., (2014); Ibrahim *et al*., (2009); Mobarak, (2010); El-Labban, (2011); Moubarak, (2013); Chieruzzi *et al*., (2013); El Gendy *et al*., (2013, 2014). The Advantage of the CCT is that interaction of soil elements with the barrette elements are taken into consideration. The proposed analysis reduces considerably the number of equations that needs to be solved. Another point of view to choose CCT for the barrette analysis is that the designer is interested in the soil settlements and contact forces are at different levels on the barrette height not at each barrette node. Using the CCT enables to apply the nonlinear response of the barrette by a hyperbolic relation between the load and settlement of the barrette.

Lately, this technique is also further developed by El Gendy *et al*., (2017) to be used for analyzing the barrette considering two cases of analyses. In the first one, the stiffness matrix of the soil is generated from flexibility coefficients with neglecting the elasticity of the barrette body. This relate to that the assumption of the analysis which considers the barrette moves as full rigid body. In the second case of analysis the entire stiffness matrix is determined from full three-dimensional Finite Element (3D FE). However, in this case, using CCT is considerably reduced the matrix, but it was still large and needs a time to be solved. Therefore, in this paper, the CCT was used for analyzing barrette. The elasticity of the barrette body was considered using the finite element method, while that of the soil elements was considered using flexibility coefficients. The compatibility between the vertical displacements of the barrette and the soil settlements at the soil-barrette interface was taken in the vertical direction only. This assumption is that the external load on the barrette head, which is expected to be heavy load, was applied in the vertical direction. For comparative examinations, the barrette elasticity is determined using either 1D or 3D finite elements. A series of examinations was carried out to verify the application for analyzing barrette by CCT

2.0 Mathematical Modeling

2.1 Soil Stiffness Matrix in Non-composed Coefficients

In non-composed coefficient method, barrette was assumed as the rectangular cross sectional shown in Figure 1. The surface of the barrette is divided into a number of shaft elements and base elements with n_s nodes, each acted upon by a distributed stress. To carry out the analysis, the stresses acting on shaft and base elements are replaced by a series of concentrated forces acting on nodes. According to El Gendy *et al*., (2017) after generating flexibility coefficients, a stiffness matrix equation of the soil in non-composed coefficients is given by:

$$\{Q\} = [ks]\{s\} \tag{1}$$

where $\{s\}$ is n_s settlement vector; $\{Q\}$ is n_s contact force vector; $[ks]$ is $n_s \times n_s$ soil stiffness matrix.

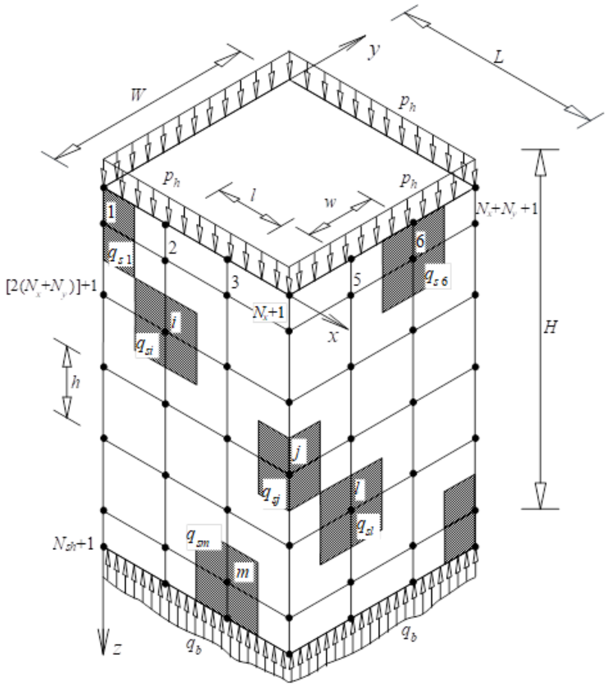

Figure 1: Barrette geometry, elements and stresses

2.2 *Barrette Stiffness Matrix Using 3D Finite Elements*

In this case, there is no approximation has to be carried out when determining the elasticity of the barrette itself due to its material, where the barrette is divided into Hexahedra solid elements. Figure 2 shows the mesh of the 3D finite elements of the barrette with loads. Each element consists of eight nodes; each node has three forces and three displacements in the three directions (*i.e.*, six degree of freedom in one node). More details concerning this type of the solid element may be found in *Chandrupatla*/ *Belegundu* (2000). The unknowns of the problem are n_s contact forces on soil-barrette interface and n_t displacements (or settlements) on all nodes of the barrette in the three directions.

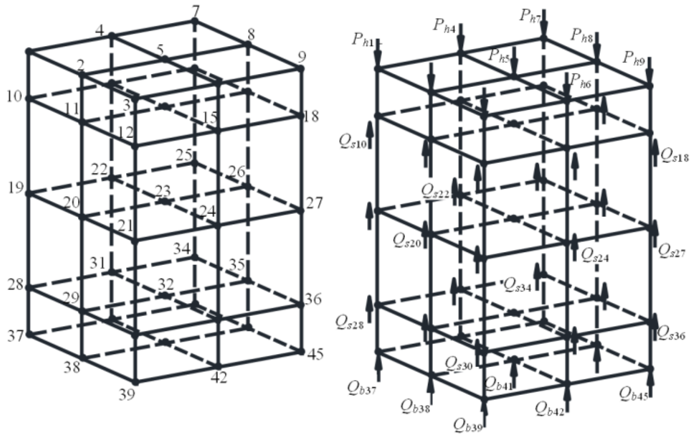

Figure 2: Mesh of the barrette with node numbering, loads and settlement

2.3 Entire Stiffness Matrix in Non-composed Coefficients

According to the principal of the finite element method, the stiffness matrix equation for the barrette can be defined as:

$$[kp]\{\delta\} = \{P\} - \{Q\} \tag{2}$$

where $\{\delta\}$ is n_t displacement vector of displacements w_i, u_i and v_i in z-, x- and y-directions; $\{P\}$ is n_h vector of applied forces on the barrette head; $\{Q\}$ is n_s vector of contact forces on the soil-barrette interface; $[kp]$ is $(n_t \times n_t)$ barrette stiffness matrix; n_h is number of nodes on the barrette head; n_s is number of nodes on the soil-barrette interface; n_t is total number of barrette nodes, $n_{t=}\ n_{h+}n_s$ Substituting Eq. (1) into Eq (2), leads to:

$$[kp]\{\delta\} = \{P\} - [ks]\{s\} \tag{3}$$

The soil stiffness matrix $[ks]$ is a full matrix, while the original size of the barrette stiffness matrix $[kp]$ is a banded matrix. Therefore, the matrix $[kp]$ is extended to be a full matrix of size $n_t * n_t$ to enable the summation process of the barrette stiffness matrix with soil stiffness matrix to be carried out.

Assuming full compatibility between barrette displacements w_i and soil settlement s_i, the following equation can be obtained:

$$[[kp] + [ks]]\{\delta\} = \{P\} \tag{4}$$

or

$$[kt]\{\delta\} = \{P\} \tag{5}$$

where [*kt*] is entire stiffness matrix of the barrette and the soil in non-composed coefficients.

Solving the above system of linear equations 5, gives the vertical displacements at each node w_i, which equal to the soil settlement s_i at that node. Substituting soil settlements from Eq. (5) into Eq. (1), gives contact forces Q_i on the barrette in case of considering the barrette as elastic body.

2.4 Soil Stiffness Matrix in Composed Coefficients

To reduce the size of the entire stiffness matrix, the CCT is used to perform a soil stiffness matrix for barrette as a line member from the original soil stiffness matrix of Eq. (1). Another point of view to choice this idea is that the designer is interested in the soil settlements and contact forces at different levels on the barrette height not at each barrette node. To describe the formulation of CCT for generating the soil stiffness matrix of the barrette in this case, consider, as an example, the simple barrette shown in Figure 3a, which has a total of n = 33 surface nodes. The barrette of 3D is converted to 1D as indicated in Figure 3b. which has n_b = 4 nodes in 4 levels. Each node has a force and a settlement in the vertical direction. The unknowns of the problem will be reduced to n_b contact forces Q_{bi} on soil-barrette interface and n_b settlements (or displacements) s_{bi} on all nodes of the barrette in the vertical direction.

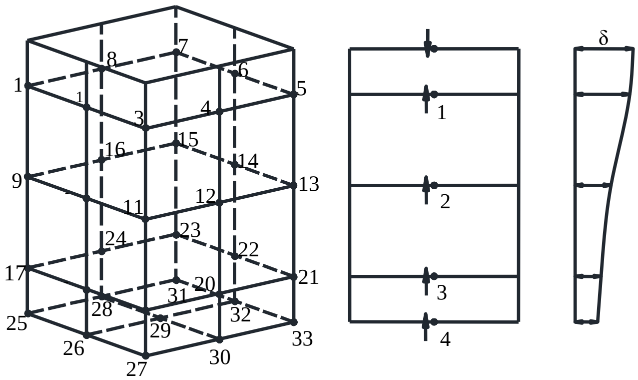

Figure 3: Surface mesh of the barrette with node numbering, loads and settlement

The soil stiffness matrix of Eq. (1) for the barrette shown in Figure 3a, which takes into account the interaction effect among all soil-barrette interface nodes, can be expanding in the following matrix equation:

$$\left\{\begin{matrix}\left\{\begin{matrix}Q_1\\ \ldots\\ Q_8\end{matrix}\right\}_1\\ \ldots\\ \left\{\begin{matrix}Q_{25}\\ \ldots\\ Q_{33}\end{matrix}\right\}_4\end{matrix}\right\}=\begin{bmatrix}k_{1,1} & \ldots & k_{1,8} & \ldots & k_{1,25} & \ldots & k_{1,33}\\ \ldots & \ldots & \ldots & \ldots & \ldots & \ldots & \ldots\\ k_{8,1} & \ldots & k_{8,8} & \ldots & k_{8,25} & \ldots & k_{8,33}\\ \ldots & \ldots & \ldots & \ldots & \ldots & \ldots & \ldots\\ k_{25,1} & \ldots & k_{25,8} & \ldots & k_{25,25} & \ldots & k_{25,33}\\ \ldots & \ldots & \ldots & \ldots & \ldots & \ldots & \ldots\\ k_{33,1} & \ldots & k_{33,8} & \ldots & k_{33,25} & \ldots & k_{33,33}\end{bmatrix}\left\{\begin{matrix}\left\{\begin{matrix}s_1\\ \ldots\\ s_8\end{matrix}\right\}_1\\ \ldots\\ \left\{\begin{matrix}s_{25}\\ \ldots\\ s_{33}\end{matrix}\right\}_4\end{matrix}\right\} \tag{6}$$

where $k_{i,j}$ is stiffness coefficient of the soil stiffness matrix, [kN/ m]. In Eq. (6), carrying out the summation of rows and columns corresponding to the barrette node *i* in 1D, leads to:

$$\left\{\begin{matrix}\left\{\sum_{i=1}^{8}Q_i\right\}_1\\ \ldots\\ \left\{\sum_{i=25}^{33}Q_i\right\}_4\end{matrix}\right\}=\begin{bmatrix}\sum_{i=1}^{8}\sum_{j=1}^{8}k_{i,j} & \ldots & \sum_{i=1}^{8}\sum_{j=25}^{32}k_{i,j}\\ \ldots & \ldots & \ldots\\ \sum_{i=25}^{33}\sum_{j=1}^{8}k_{i,j} & \ldots & \sum_{i=25}^{33}\sum_{j=25}^{33}k_{i,j}\end{bmatrix}\left\{\begin{matrix}s_{b1}\\ \ldots\\ s_{b4}\end{matrix}\right\} \tag{7}$$

Accordingly, Eq. (7) of soil stiffness matrix can be rewritten for the barrette of 1D in composed coefficients as:

$$\left\{\begin{matrix}Q_{b1}\\ Q_{b2}\\ Q_{b3}\\ Q_{b4}\end{matrix}\right\}=\begin{bmatrix}K_{1,1} & K_{1,2} & K_{1,3} & K_{1,4}\\ K_{2,1} & K_{2,2} & K_{2,3} & K_{2,4}\\ K_{3,1} & K_{3,2} & K_{3,3} & K_{2,4}\\ K_{4,1} & K_{4,2} & K_{4,3} & K_{2,4}\end{bmatrix}\left\{\begin{matrix}s_{b1}\\ s_{b2}\\ s_{b3}\\ s_{b4}\end{matrix}\right\} \tag{8}$$

where $K_{i,j}$ is composed coefficient, [kN/m]; s_{bi} is settlement in node *i* of 1D barrette, [m], $s_{b1} = s_1 = s_2 = \ldots = s_8$, $s_{b2} = s_9 = s_{10} = \ldots = s_{16}$, ..., $s_{b4} = s_{25} = s_{26} = \ldots = s_{33}$; Q_{bi} is contact force on node *i* of 1D barrette [kN], $Q_{b1} = Q_1 + Q_2 + \ldots + Q_8$, $Q_{b2} = Q_9 + Q_{10} + \ldots + Q_{16}$, ..., $Q_{b4} = Q_{25} + \ldots + Q_{33}$. Eq. (8) show that the soil stiffness matrix in Eq. (6) of size 33×33 is reduced considerably to an equivalent soil stiffness matrix of size 4×4. It could be written in a compacted matrix form in composed coefficients as:

$$\{Q_b\}=[kb]\{s_b\} \tag{9}$$

2.5 Barrette Stiffness Matrix Using 1D Finite Elements

To generate a barrette stiffness matrix compatible with the above composed soil stiffness matrix, the barrette is represented by a vertical line member having a variable settlement (or vertical displacement) along its height.

Using 1D finite element method in the analysis of barrette, only the axial compression of the barrette is considered in determining displacements of barrette elements. The beam stiffness matrix of the barrette element *i* can be expressed as (Figure 4):

$$[kp]_i = \frac{Ep \cdot Ap_i}{l_i}\begin{bmatrix} 1 & -1 \\ -1 & 1 \end{bmatrix} \tag{10}$$

where *Ep* is Modulus of Elasticity of the barrette material, [kN/m^2]; Ap_i is cross-section area of the barrette element *i*, [m^2]; l_i is length of the barrette element *i*, [m].

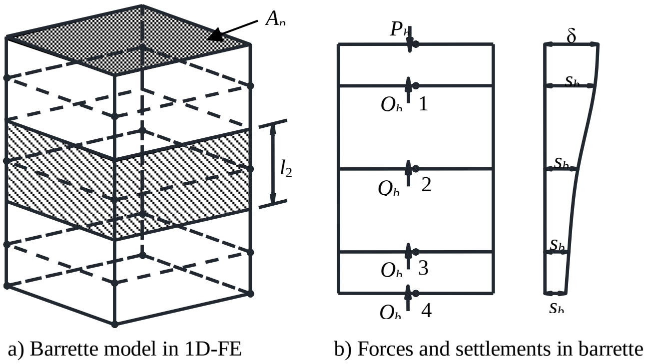

Figure 4: Finite element mesh of barrette and element geometry

2.6 *Entire Stiffness Matrix in non-composed Coefficients*

According to the principal of the finite element method, the assembled axial stiffness matrix equation for the barrette can be written as:

$$[kp]\{\delta\} = \{P\} - \{Q_b\} \tag{11}$$

where $\{\delta\}$ is (n_s+1) displacement vector; $\{P\}$ is (n_s+1) vector of applied load on the barrette, $\{P\} = \{Ph, o, o, o, \ldots, o\}^T$; $[kp]$ is $(n_s+1)\times(n_s+1)$ beam stiffness matrix. Substituting Eq. (9) into Eq (11), leads to:

$$[kp]\{\delta\} = \{P\} - [kb]\{s_b\} \tag{12}$$

Assuming full compatibility between barrette displacement δ_i and soil settlement s_{bi}, the following equation can be obtained:

$$\left[[kp] + [kb]\right]\{\delta\} = \{P\} \tag{13}$$

or

$$[ktb]\{\delta\}=\{P\} \tag{14}$$

where [*kt*b] is entire stiffness matrix of the barrette and the soil in composed coefficients.

Solving the above system of linear equations 14, gives the displacement Sb_i at each barrette level, which equal to the soil settlement at that node. Substituting soil settlements from Eq. (14) into Eq. (9), gives contact forces Q_{bi} on the barrette. To get the contact forces Q_i on all barrette nodes on the 3D model in Figure 3a, substituting soil settlements from Eq. (14) into Eq. (6).

3.0 Numerical Results

The proposed method for analyzing barrette using CCT outlined in this paper was implemented in the program ELPLA. With the help of this program, an analysis of two verification examples is carried out first to judge the proposed method for nonlinear analyses. Then, a comparative examination of modeling for analyzing single elastic and rigid barrette is carried out.

3.1 Validity of linear Analysis of Single Barrette

An analytical analysis of a single barrette having a rectangular cross section embedded in a multi-layered soil medium is available in the reference Basu *et al.*, (2008). In the analytical analysis, the differential equations governing the displacements of the barrette-soil system were obtained using variation principles. Closed-form solutions for barrette deflection and axial force along the barrette shaft were then produced by using the method of initial parameters.

The barrette is considered and analyzed for four different cases under different loads, geometries and subsoil conditions. The load on the barrette head and barrette geometry for the chosen cases are listed in Table 1. The subsoil of each case consist of four layers, each layer has a different Modulus of Elasticity, E_s and *Poisson's* ratio, ν_s as listed in Table 3. The barrette material properties are listed in Table 2.

Table 1: Loads and barrette geometries.

Case	*Load [kN]*	*Height [m]*	*Cross section*
1	3000	15	0.5 [m] × 0.5 [m]
2	2500	10	0.7 [m] × 0.7 [m]
3	10000	40	2.8 [m] × 0.8 [m]
4	8000	30	2.7 [m] × 1.2 [m]

Table 2: Barrette material properties.

Modulus of Elasticity of the barrette material	$E_c = 2.5\times10^7$ [kN/m^2]
Poisson's ratio of the barrette material	$\nu_c = 0.20$ [-]

Table 3: Subsoil properties.

Case	*Layer No.*	*z [m]*	*E_s [kN/m^2]*	*ν_s [-]*
1	1	2	10000	0.40
	2	5	15000	0.35
	3	10	30000	0.30
	4	∞	100000	0.15
2	1	1	10000	0.40
	2	5	15000	0.35
	3	8	30000	0.30
	4	∞	80000	0.20
3	1	5	20000	0.35
	2	15	25000	0.30
	3	35	30000	0.30
	4	∞	80000	0.20
4	1	2	15000	0.40
	2	12	25000	0.30
	3	22	30000	0.30
	4	∞	100000	0.15

A comparison of results of the single barrette in a multi-layered soil medium of the present analysis using flexibility coefficient with those of Basu *et al.,* (2008) is presented herein. The height of the barrette is divided into equal elements, and the height of each element is h = 1 [m] in all cases. Both the barrette length and width are divided into four equal elements in each case. In the analysis, barrette material is considered to be elastic and the barrette is analyzed as 1D finite elements.

The barrette settlement, s along the barrette height obtained from the present analysis using flexibility coefficient for the four cases of analysis are compared with those of Basu *et al.*, (2008) in Figure 5 to Figure 8.

From these results, it can be concluded that the absolute difference between the maximum settlements is ranging between 0.8 % for the first case and 2.0 % for the second case, while the other cases it is only 1.0 %. Also, the absolute differences between the minimum settlements are 7.0 %, 4.0 %, 15.0 % and 5.0 % respectively.

These results show also that verification results of the present analysis using flexibility coefficient are in good agreement with those of Basu *et al.*, (2008). Results of the barrette head settlements are similar to those of *Basu et al.*, (2008). However, regarding results of the base settlements, the difference reached 15.0 % in case of a barrette having a great aspect ratio in the cross section, case (3). The difference in this case is very small when compared to the barrette dimensions, which equals to 0.06 cm.

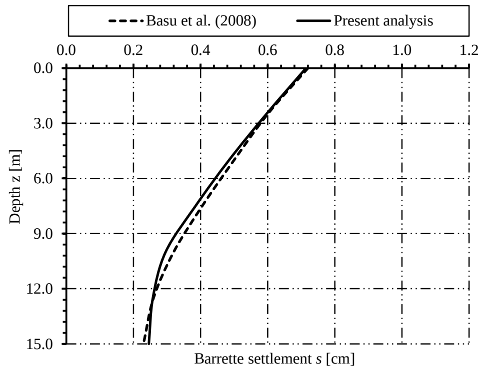

Figure 5: Settlement along the barrette height (case 1).

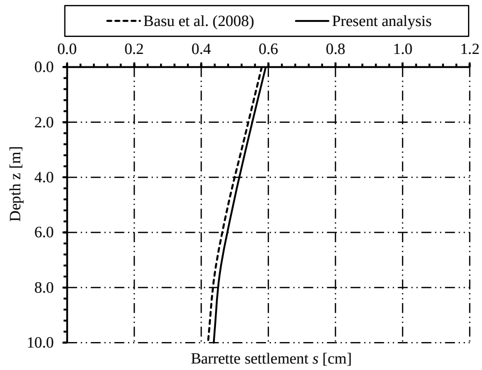

Figure 6: Settlement along the barrette height (case 2).

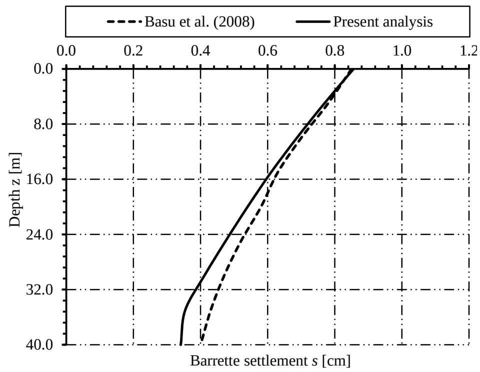

Figure 7: Settlement along the barrette height (case 3).

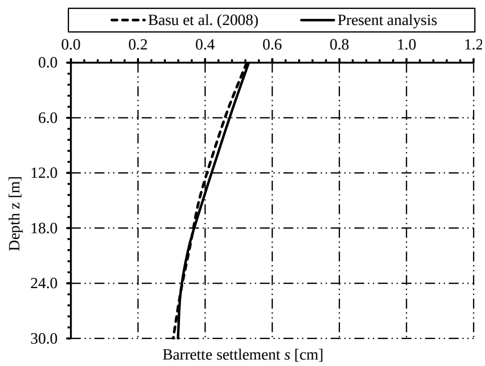

Figure 8: Settlement along the barrette height (case 4).

3.2 Case Studies of a Single Barrette

This section presents the main features of the numerical models used in analyzing the behavior of single barrette in a real subsoil. The subsoil of East Port Said area is considered as the proposed real subsoil in these case studies. The reason is that the existing heavy loaded structures in East Port Said suffered from settlement problems due to the presence of extended soft clay layers. The typical subsoil layers of East Port Said area, as presented by *Hamza et al.*, (2000). in Table 7, is considered in the analysis. The different case studies under investigation are also described. Every case is examined in a parametric study. The study covered different barrette lengths L with different barrette heights H for a constant barrette width W of 1.0 m. The effect of these variables on the barrette loads at certain settlement is also investigated. Furthermore, the analysis is carried out considering various calculation methods. The main features of the most effective numerical methods suitable for the single barrette analysis in East Port Said clay are also discussed. The main variables of the parametric study are described in the next paragraphs.

Twelve case studies of single barrettes are considered as given in Table 4.

Table 4: Studied cases of a single barrette.

Length/Height	*L = 1.5*	*L = 2.0*	*L = 2.5*	*L = 3.0*
H = 24	Case 1	Case 2	Case 3	Case 4
H = 30	Case 5	Case 6	Case 7	Case 8
H = 36	Case 9	Case 10	Case 11	Case 12

The subsoil of each case assumed to be the typical soil properties of East Port-Said area as given in Table 6, each layer has a different Modulus of Elasticity E_s and *Poisson's* ratio ν_s. The barrette material properties are listed in Table 5.

Table 5: Barrette material properties.

Modulus of Elasticity of the barrette material	$E_c = 2.5\times10^7$	[kN/m^2]
Poisson's ratio of the barrette material	$\nu_c = 0.20$ [-]	

Table 6: Subsoil properties, *Hamza et al.* [9].

Layer No.	*z [m]*	*E_s [kN/m^2]*	*ν_s [-]*
1	5	2400	0.2
2	13.5	30000	0.25
3	28.5	8120	0.2
4	38.5	9940	0.2
5	48.5	11340	0.2
6	58.5	12810	0.2
7	92.5	60000	0.2
8	120	144000	0.2

In this paper, comparative tests of numerical models for analyzing single barrette in East Port Said deep clay layers are performed. For the purpose of comparative investigations, two different models of single barrette are considered in a total of 48-case studies. The analysis is carried out by the following methods:

1. Elastic barrette in a continuum soil medium.
2. Rigid barrette in a continuum soil medium.

The load-settlement relation is determined according to:

a) Nonlinear analysis of a single barrette using hyperbolic function.
b) Linear analysis of a single barrette.

The availability of the above mentioned analysis methods and load-settlement models provides the researcher with a wide variety of numerical models that can handle the problem of single barrette as indicated in Table 4. In this analysis, many case studies of single barrette are analyzed using different numerical models in order to explore the effect of the type of calculation method on the results.

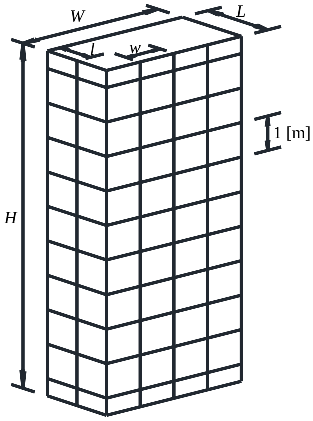

Figure 9: Surface element of the single barrette.

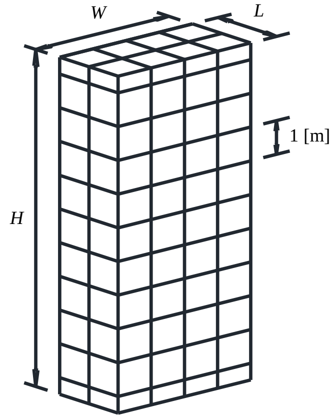

Figure 10: Barrette representing by 3D finite elements.

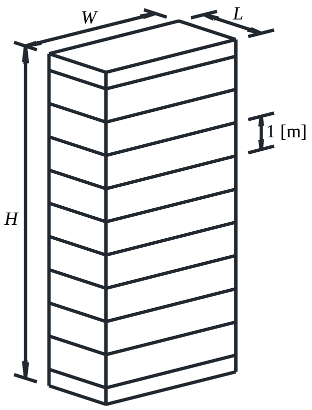

Figure 11: Barrette representing by 1D finite elements.

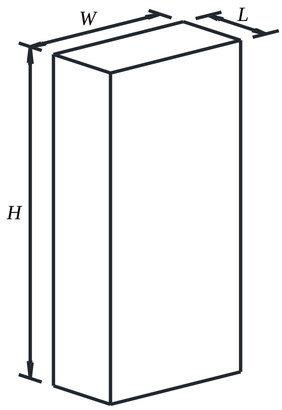

Figure 12: Barrette representing as rigid elements.

Twelve case studies are presented with variables including; the height, length and width of the barrette which are divided into equal elements, and the height of each element is h = 1.0 m, in all cases. Both the barrette length and width were divided into equal elements, the length and the width of each element is l = w = 0.5 m, in all cases as shown in Figure 9 to Figure 12.

3.2.1 Limit Barrette Load

A limit barrette load Ql kN has been used as parameter geometry for the hyperbolic curve of nonlinear response of load settlement relation. Russo (1998) suggested limit shaft friction not less than ql = 180 kN/m^2 meeting undrained shear strength of 200 kN/m^2. To carry out the present analysis a limit shaft friction of ql = 180 kN/m^2 has been assumed, the limit barrette load considered in the analysis for barrette dimensions which are presented in Table 7.

Table 7: Limit barrette load Q_l [kN] for different barrette geometries.

Length/Height	*L = 1.5*	*L = 2.0*	*L = 2.5*	*L = 3.0*
H = 24	21600	25920	30240	34560
H = 30	27000	32400	37800	43200
H = 36	32400	38880	45360	51840

3.2.2 Guideline of Barrette Stiffness

One of the difficulties that arise when analyzing a three dimensional problem, such as barrette in a continuum soil medium, is the huge number of 3D finite elements required for the analysis. Consequently, a long computational time is needed. Before performing the analysis routine, an examination for the used element type and barrette rigidity is carried out. This examination depends on that barrette itself as a great block of concrete which may be considered as rigid enough in the long direction. This property advantage maybe used to simplify the problem and to accelerate the analysis.

3.2.2.1 Barrette Elasticity

To analyze the barrette as an elastic material, two different methods are used in this paper. The first depends on 3D finite elements representing the barrette by its natural geometry, Figure 10. The second method using 1D finite elements in the z-direction representing the barrette as line elements in the direction of its height, Figure 11. The twelve cases listed before are analyzed using the two different types of elements, and the results of reactions, settlements and elapsed time are compared, as shown in Figure 13 to Figure 16.

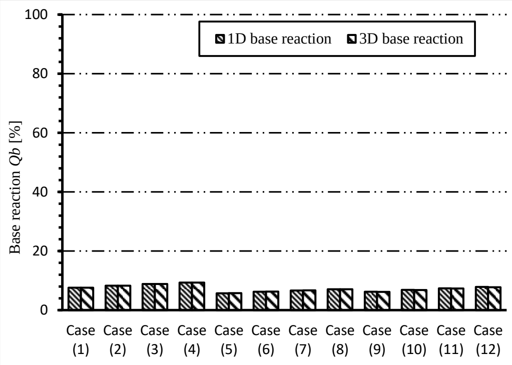

Figure 13: Base reaction using 1D and 3D finite elements.

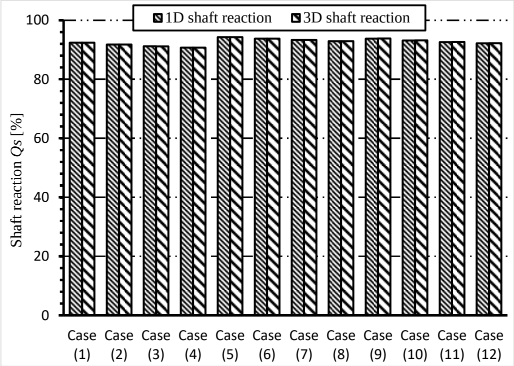

Figure 14: Shaft reaction using 1D and 3D finite elements.

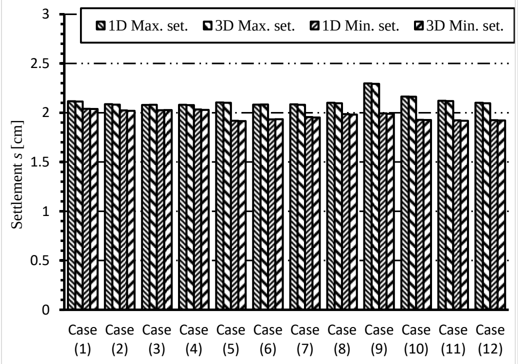

Figure 15: Max. and Min. settlement when using 1D and 3D finite elements.

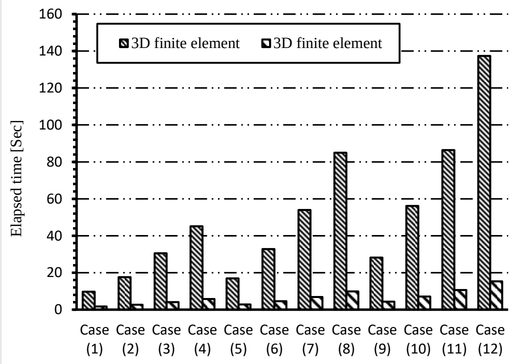

Figure 16: Elapsed time [sec] when using 1D and 3D finite elements.

From Figure 13 to Figure 16 it can be concluded that:

- The elapsed time to analyze the single barrette will be decreased by about 85 % when using 1D finite elements.
- The difference in the settlement when using 1D and 3D finite elements are less than 0.25 %.

3.2.2.2 Barrette Rigidity

Settlement along the barrette height is considered the main important value in all barrette results. Therefore, in this section an examination is carried out for considering the barrette as one unit having a uniform settlement along its height or as an elastic body having a non-uniform settlement along its height. In the first assumption the barrette is treated as a full rigid body which obeys the rigid body movement, while in the second the barrette is treated as an elastic body considering the elastic property of its material.

The twelve cases listed before for single barrette are analyzed as a full rigid barrette in a continuum soil medium, Figure 12, and as an elastic barrette in a continuum soil medium, Figure 11. Results of the settlements are compared using both linear and nonlinear analyses, as shown in Figure 17 and Figure 18.

From Figure 17 and Figure 18, it can be concluded that:

- The absolute difference between the maximum settlement considering a rigid barrette and an elastic barrette for both linear and nonlinear analyses is about 9.74 %. It occurred in case (9), and is less than 8 % in all the remaining other cases.
- The absolute difference between the minimum settlement considering a rigid barrette and an elastic barrette for both linear and nonlinear analyses is about 4.78 %. It is occurred in case (9), and is less than 4 % in the other cases.
- The maximum difference occurs in barrettes having a long height in the soil.
- Barrettes of small cross sections gave higher settlement difference.
- In spite of the relatively large differences between the maximum settlements which ranged between 9.74 % and 4.78 %, their actual values are very small, 0.204 cm and 0.1 cm, respectively.

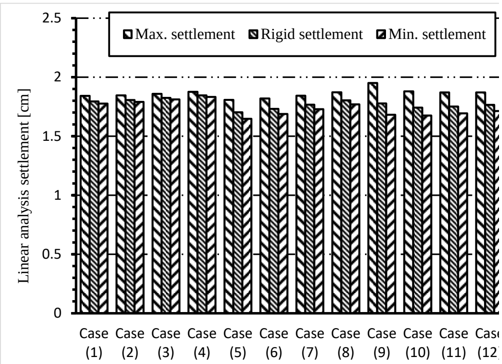

Figure 17: Maximum, minimum and rigid settlement using linear analysis

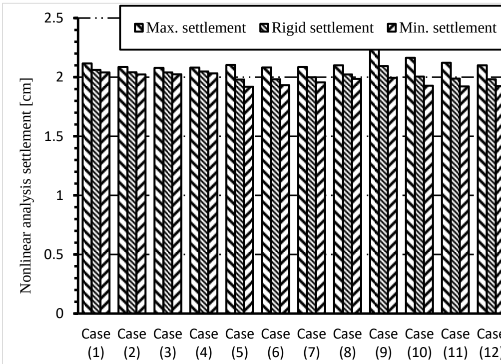

Figure 18: Maximum, minimum and rigid settlement using nonlinear analysis

4.0 Conclusions

An application of *CCT* on barrettes as large-section supports is presented. The proposed technique considers the 3D full interactions between barrette and soil. From application of *CCT* technique on real soil, it can be concluded that:

- Both flexibility coefficient and 3D finite element models can be used safely in the linear analysis of single barrette in cases of half space soil and soil consists of different layers extended from weak to hard layers and the results are identical.
- For soils that consist of different layers extended from hard layer to weak one, the maximum difference in the settlement between both models is high and reach twice. It is found that settlements from 3D finite element model are less than those of flexibility coefficient model. This is related to, in 3D finite element mode, the first harder layer is to act as a support for the next weaker soil layer, where the soil is treated as continuum structure connected together and maybe resist soil tension. In this case interface elements between the two layers maybe inserted to enhance the results.
- Flexibility coefficient model can be used safely to model all cases of soil conditions.
- Due to the less number of nodes in flexibility coefficient model rather than 3D finite element model, the first model consumes less computation time in the analysis.
- Treating the barrette as an elastic body and representing the barrette by either 1D or 3D finite elements, gives nearly the same results. This conclusion is used in this paper, when analyzing the barrette as an elastic body.
- For these cases, treating the barrette as a rigid body due to its high rigidity in the direction of its height, gives nearly the same results as treating it as an elastic body.

References

Basu, D., Prezzi, M., Salgado, R., Chakraborty, T. (2008). *Settlement analysis of piles with rectangular cross sections in multi-layered soils*. Computers and geotechnics 35: 563-575.

Chandrupatla, T., Belegundu, A. (2000). *Introduction to Finite Elements in Engineering Prentice*. Hall of India, New Delhi.

Chieruzzi, G., Roy, D., Ayoubian, A. (2013). *Measured and Modeled Settlement of Power Plant on Piled Raft Foundation*. DIF, 37th Annual Deep Foundations Conference, Houston, TX.

El Gendy, M. (2007). *Formulation of a composed coefficient technique for analyzing large piled raft*. Ain Shams Engineering Journal 42: 29-56.

El Gendy, M., El Araby, I., Kamal, M. (2013). *Comparative Examination of Single Bored Piles Using International Codes*. Scientific Research Journal of Engineering 5: 796-806.

El Gendy, M., El Araby, I., Kamal, M. (2014). *Comparative analysis of large diameter bored piles using international codes*. Deep Foundations Institute Journal 8: 15-26.

El Gendy, M., El Gendy, A. (2017). *Analysis and design of raft and piled Raft-Program ELPLA*. GEOTEC Software Inc., Canada.

El Gendy, M., Ibrahim, H., El Araby, I. (2017). *ANALYZING SINGLE BARRETTES AS RIGID SUPPORT BY CCT*. Malaysian Journal of Civil Engineering 29 (3): 273-288.

El Labban, A. (2011). *Comparative Studies for Piled Raft Resting on Port Said Clay*. M.Sc. Thesis. Port Said University.

Fellenius, B., Altaee, A., Kulesza, R., Hayes, J. (1999). *O-Cell testing and FE analysis of 28-m-deep barrette in Manila, Philippines. Journal of Geotechnical and Environmental Engineering* 125: 566-575.

Hamza, M., Hamed, H. (2000). *Three Dimensional Soil-Structure Analysis of Port-Said East Quay Wall*. Maritime Engineering and Ports II, C.A. Brebbia & J. Olivella, ISBN 1-85312-829-5.

Hattab,F.(2007). *Vergleichende Untersuchungen numerischer Modelle für die Berechnung von Pfahlplattengründungen*. Diplomarbeit, Matr. NIVERSITÄT SIEGEN.

Ibrahim, F., El Gendy, M., Salib, R., El Kamash, W. (2009). *Nonlinear analysis of piled raft with 3D-space structure*. Port-Said Engineering Research Journal 13.

Kamash, W. (2009). *Analysis of Structures on Piled Raft under Earthquake Excitations*. Ain Shams Journal of Civil Engineering 1: 203-2141.

Kamash, W. (2012). *The positioning and thickness effect for soft clay layer on 3D-building resting on piled raft*. Ain Shams Engineering Journal 3: 17–26.

Kamash, W., El Gendy, M., Salib, R., Kandil, M. (2014). *Studying of Shear Walls with Piled Raft over Soft Soil against Seismic Loads*. Port Said Engineering Research Journal 18: 144-152.

Lei, G., Hong, X., Shi, J. (2007). *Approximate three-dimensional analysis of rectangular barrette-soil-cap interaction*. Can. Geotechnical Journal 44: 781-796.

Lin, S., Lu, F., Kuo, C., Su, T., Mulowayi, E. (2014). *Axial capacity of barrette piles embedded in gravel layer*. Journal of GeoEngineering 9: 103-107.

Mobarak, W. (2010). *Effect of tie girders on pile caps in Port Said*. M.Sc. Thesis, Faculty of Engineering. Suez Canal University. Port Said.

Moubarak, A. (2013). *Analysis of Flexible Retaining Walls and Piled Rafts as Settlement Reducer in Port-Said.* PhD thesis, Port Said university.

Plaxis Bulletin. Issue 32/ autumn 2012. Delft. The Netherlands.

Rabiei, M. (2009). *Parametric Study for Piled Raft Foundations*. EJGE 14.

Rabiei, M. (2010). *Effect of Pile Configuration and Load Type on Piled Raft Foundations Performance*. Deep Foundations and Geotechnical Institute Testing (ASCE-GSP 205: 34-41.

Rabiei, M. (2016). *Piled Raft Design Strategies for High Rise Buildings*. Geotechnical and Geological Engineering 34: 75-85.

Reda A. (2009). *Optimization of reinforced concrete piled raft*. M.Sc. Thesis, Faculty of Engineering. Suez Canal University. Port Said.

Russo, G. (1998). *Numerical analysis of piled rafts*. International Journal for Numerical and Analytical Methods in Geomechanics 22: 477-493.

Seo, H., Basu, D., Prezzi, M., Salgado, R. (2009). *Load-settlement response of rectangular and circular piles in multilayered soil*. Geotechnical and Geoenvironmental Eng: 420-430.

Shulyatiev, O., Dzagov, A., Bokov, I., Shuliatev S. (2013): *Correction of soil design parameters for the calculation of the foundation based on the result of barrettes static load test*. 18th International Conference on Soil Mechanics and Geotechnical Engineering. Paris: 614-618.

Thasnanipan, N., Maung, A. and Tanseng, P. (1998). *Barrettes Founded in Bangkok Subsoils, Construction and Performance*. Proceedings of the Thirteenth Southeast Asian Geotechnical Conference: 573-578.

Thasnanipan, N., Maung, A. and Aye, Z. (2001): *Record load test on a large barrette and its performance in the layered soils of Bangkok*, 5th International conference on deep foundation practice incorporating Piletalk. Singapore: 363-370.